

## B-site doping effects of $\text{NdBa}_{0.75}\text{Ca}_{0.25}\text{Co}_2\text{O}_{5+\delta}$ double perovskite catalysts for oxygen evolution and reduction reactions

Nam-In Kim <sup>a,†</sup>, Sung-Hwa Cho <sup>a,†</sup>, Se Hwan Park <sup>b</sup>, Young Joo Lee <sup>b</sup>, Rana Arslan Afzal <sup>a</sup>, Jeseung Yoo <sup>a</sup>, Young-Soo Seo <sup>a</sup>, Yun Jung Lee <sup>b, \*\*</sup>, Jun-Young Park <sup>a, \*</sup>

### Supplementary Figures

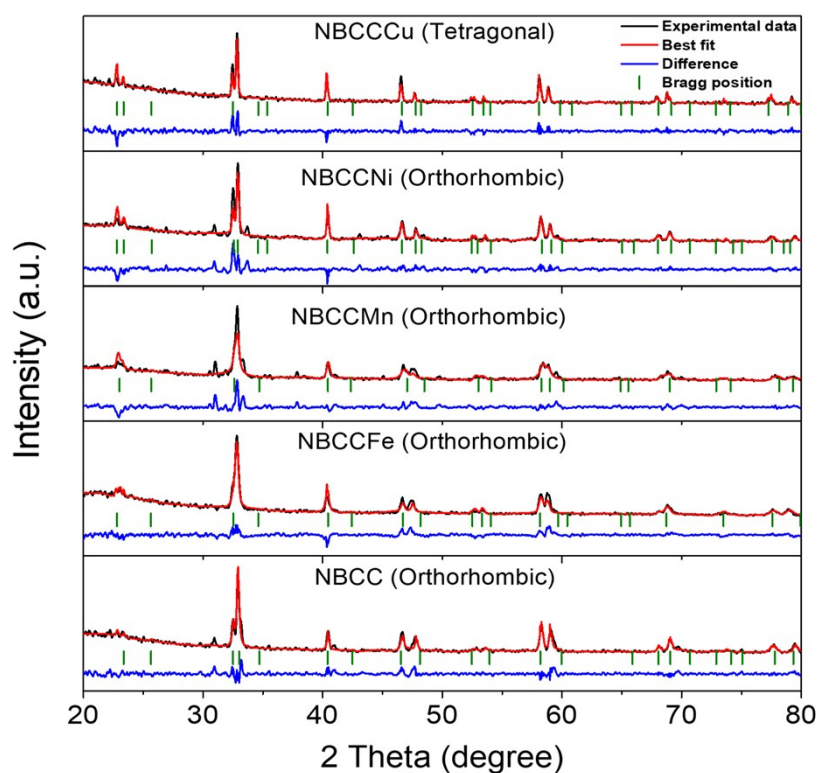


Fig. S1. Rietveld refinements of NBCC-based catalysts processed by the Fullprof program.

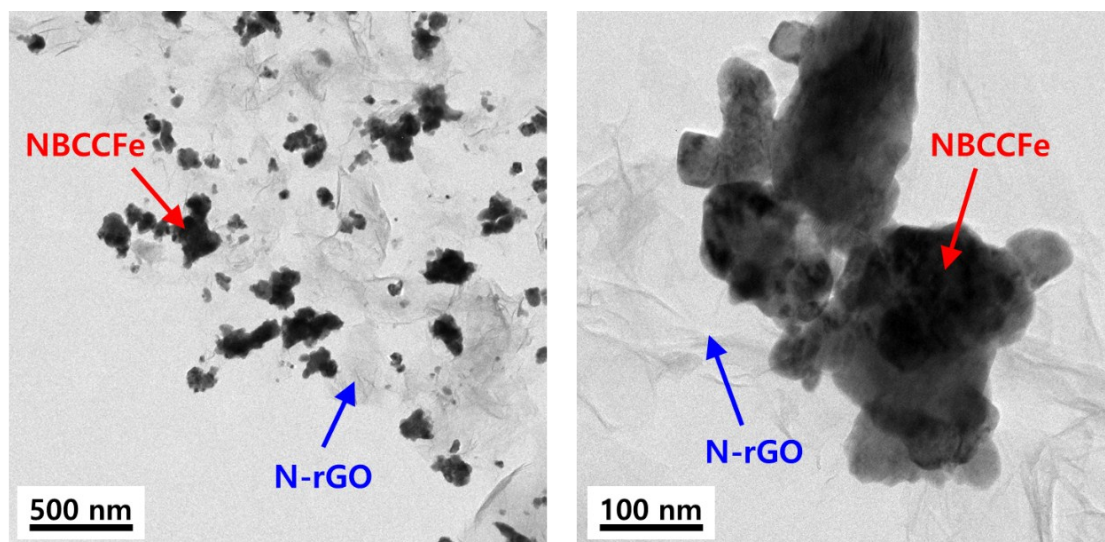


Fig. S2. Morphological characteristics of NBCCFe/N-rGO hybrid catalyst analyzed by HRTEM.

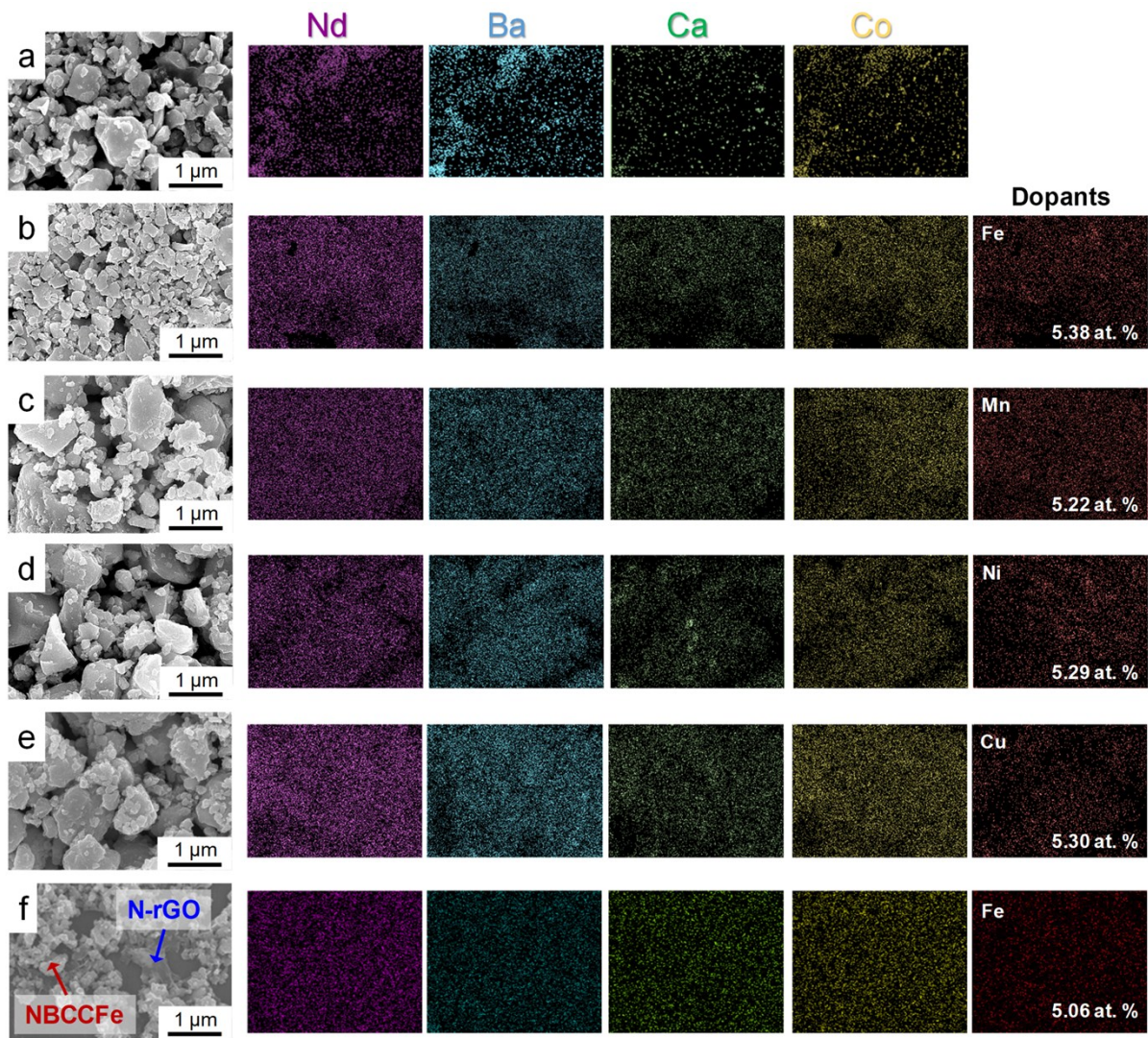


Fig. S3. Surface morphology and distribution of elemental compositions of catalysts by FE-SEM and EDX mapping: (a) NBCC (b) NBCCFe (c) NBCCMn (d) NBCCNi, (e) NBCCCu, and (f) NBCCFe/N-rGO.

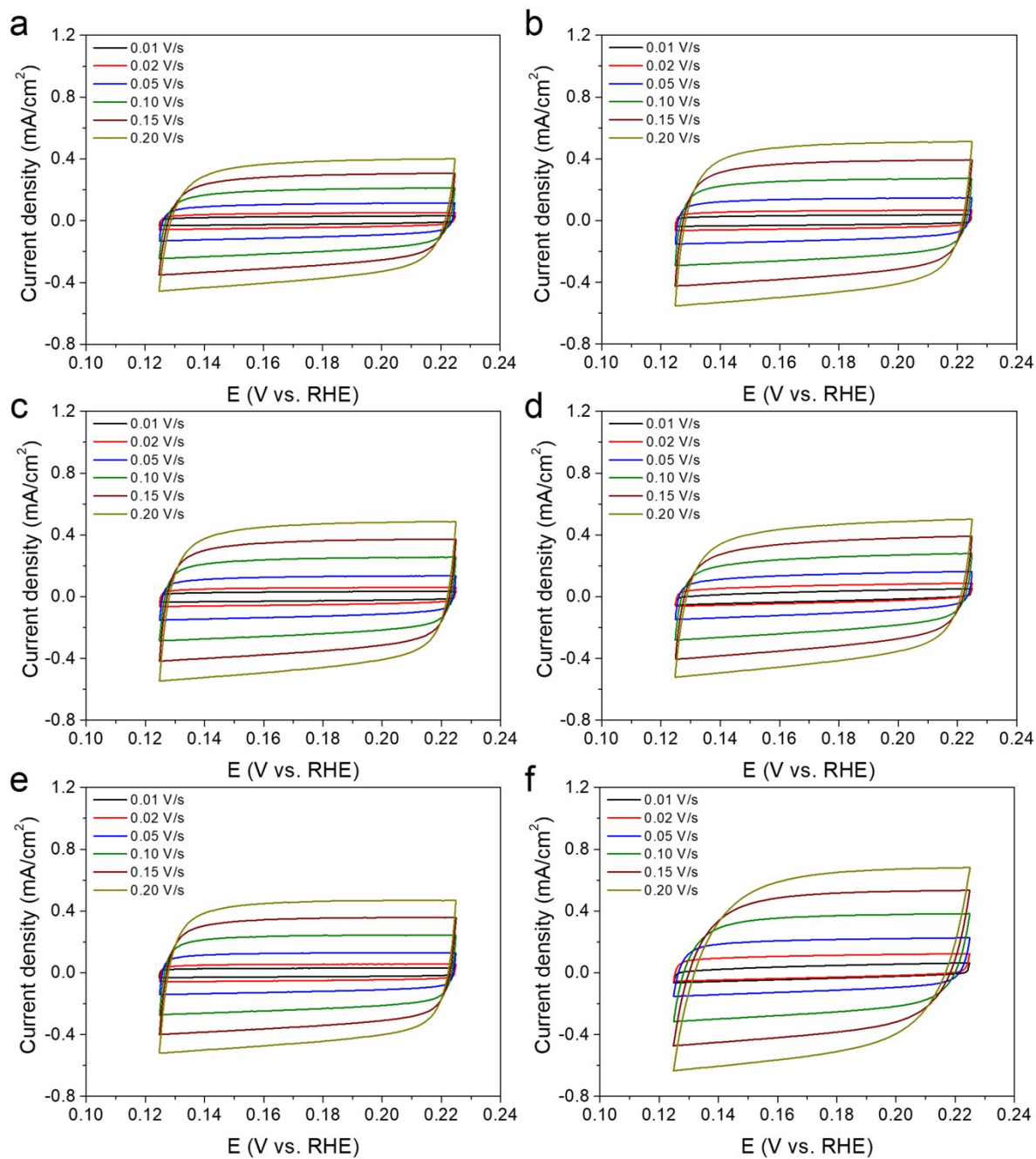


Fig. S4. Cyclic voltammogram curves of the catalysts with different scan rates (10-200  $\text{mV}\cdot\text{s}^{-1}$ ). (a) NBCC, (b) NBCCFe, (c) NBCCMn, (d) NBCCNi, (e) NBCCCu, and (f) NBCCFe/N-rGO.

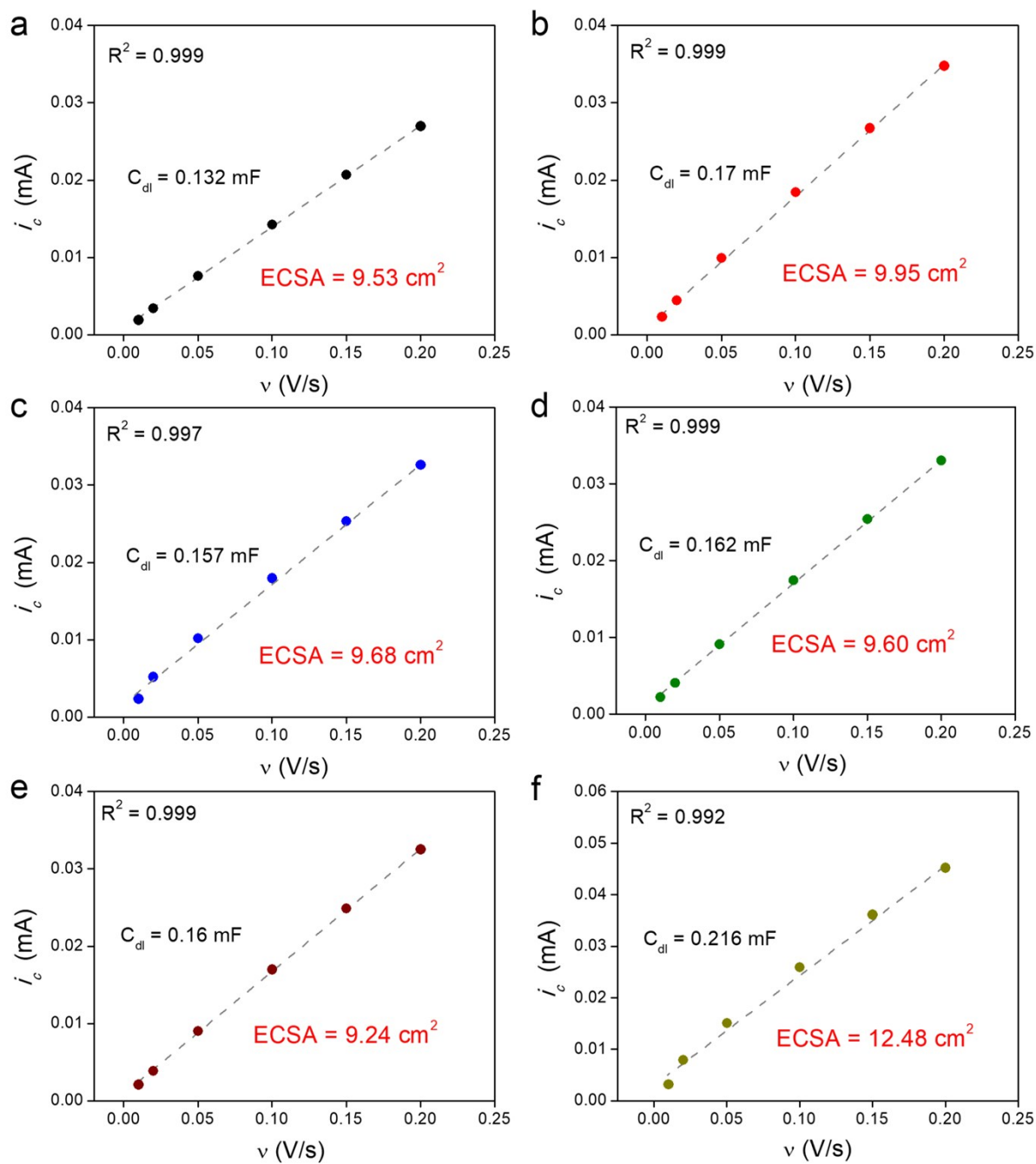


Fig. S5. Linear plots for the measured charging current ( $i_c$ ) versus scan rate for calculation of the ECSA. (a) NBCC, (b) NBCCFe, (c) NBCCMn, (d) NBCCNi, (e) NBCCCu, and (f) NBCCFe/N-rGO. Double layer capacitances of the materials were determined from the linear plots.

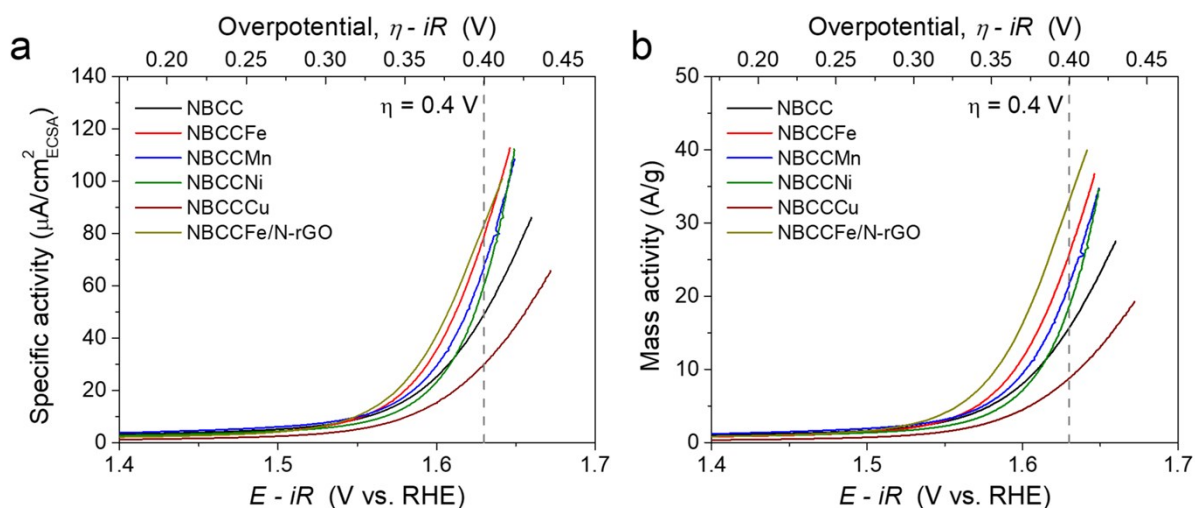


Fig. S6. (a) Specific activity ( $\mu\text{A}\cdot\text{cm}^{-2}_{\text{ECSA}}$ ) and (b) mass activity ( $\text{A}\cdot\text{g}^{-1}$ ) of catalysts in OER polarization curves normalized by the ECSA at  $\eta = 0.4\text{ V}$  in  $0.1\text{ M KOH}$  solution.

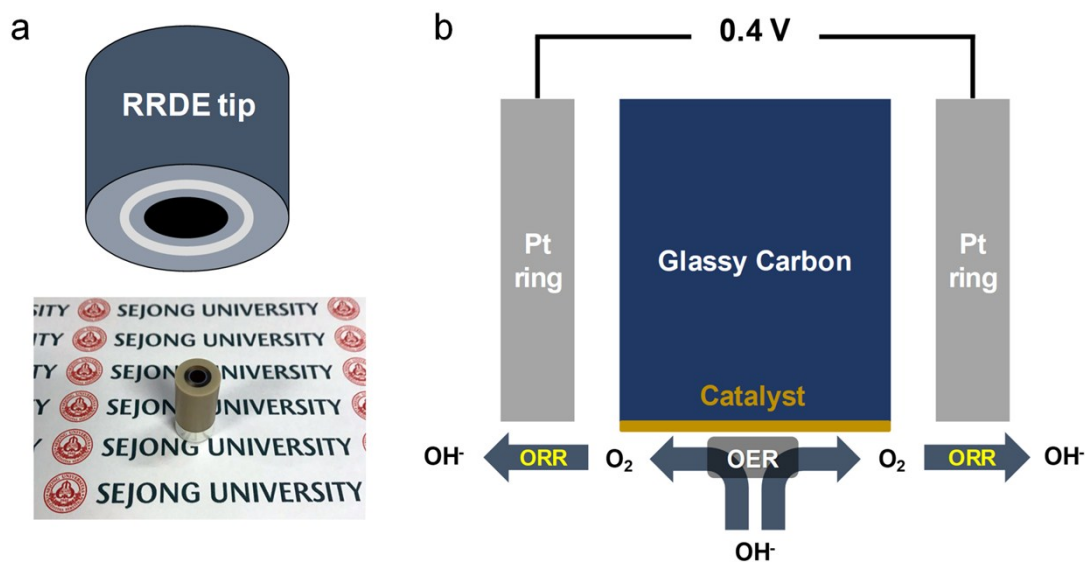


Fig. S7. (a) Schematic illustration (top) and Actual photograph (bottom) of the RRDE tip. (b) The continuous OER (disk) to ORR (ring) process initiated on a RRDE ( $\text{N}_2$ -saturated  $0.1\text{ M KOH}$ , ring potential:  $0.40\text{ V}$ ).

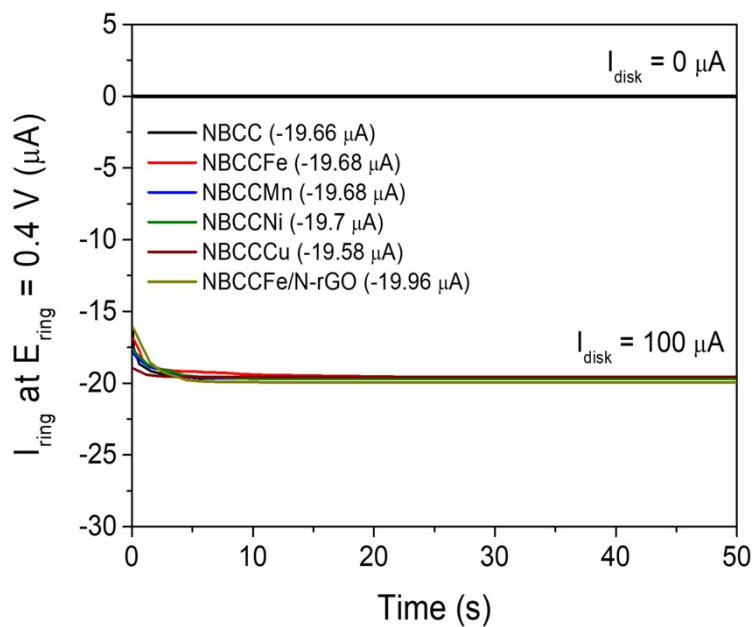


Fig. S8. The ring currents of NBCC-based catalysts on a RRDE (1,600 rpm) in 0.1 M KOH solution (ring potential: 0.40 V).

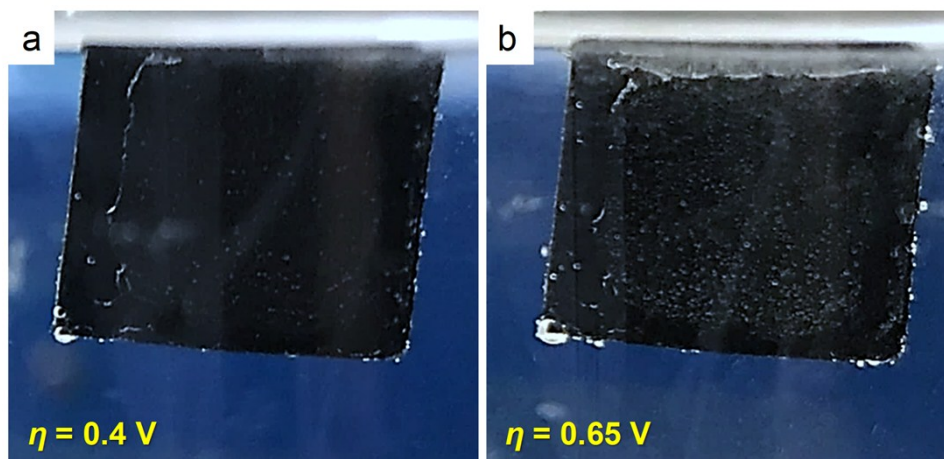


Fig. S9. Images of oxygen bubble generation in a large-scale water electrolysis half-cell (1 cm<sup>2</sup>) using the NBCCFe catalyst at  $\eta = 0.4$  V (left) and  $\eta = 0.65$  V (right).

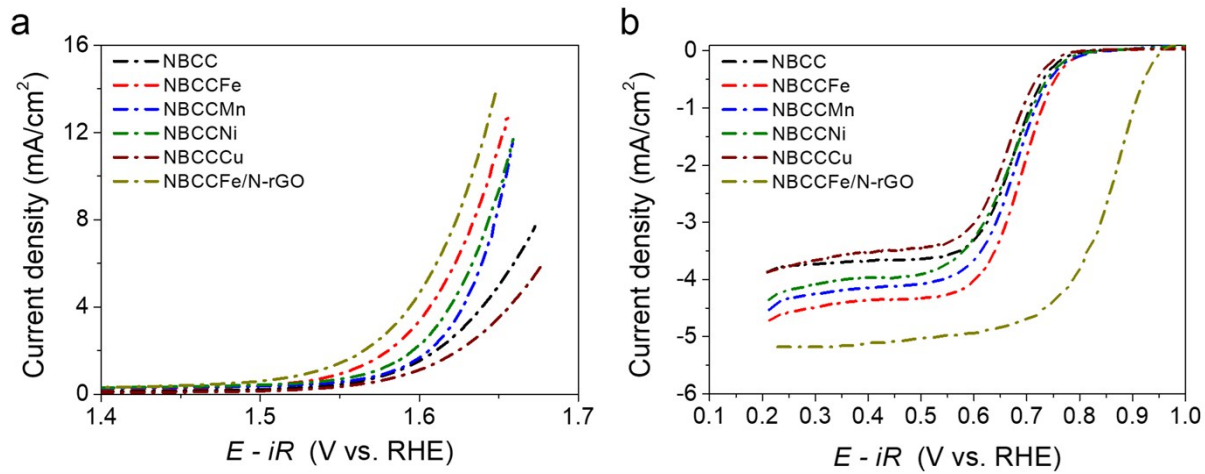


Fig. S10. 1,500<sup>th</sup> OER polarization curves and 10,000<sup>th</sup> ORR polarization curves of NBCC and doped-NBCC catalysts.

## 2. Supplementary Tables

Table S1. Comparison of oxygen activity of NBCCFe and NBCCFe/N-rGO with reported perovskite-based electrocatalysts.

Catalysts	$E_{\text{ORR}}$ (V) at $j = -3$ $\text{mA cm}^{-2}$	$E_{\text{OER}}$ (V) at $j = 10$ $\text{mA cm}^{-2}$	Oxygen activity <sup>a</sup> (V)	Reference
NBCCFe/N-rGO	0.848	1.609	0.761	This Work
NBCCFe	0.679	1.627	0.948	This Work
Core-Corona LaNiO <sub>3</sub> /N-CNT	0.64	1.67	1.03	Nano Lett. 2012, 12, 1946 (Ref. 1)
La <sub>0.3</sub> (Ba <sub>0.5</sub> Sr <sub>0.5</sub> ) <sub>0.7</sub> Co <sub>0.8</sub> Fe <sub>0.2</sub> O <sub>3-<math>\delta</math></sub> /KB	0.58	1.59	1.01	Angew. Chem. Int. Ed. 2014, 53, 4582 (Ref. 2).
porous CaMnO <sub>3</sub>	0.8	1.81	1.01	Adv. Mater. 2014, 26, 2047 (Ref. 3).
Ar treated Ba <sub>0.5</sub> Sr <sub>0.5</sub> Co <sub>0.8</sub> Fe <sub>0.2</sub> O <sub>3</sub> /KB	0.62	1.77	1.05	Adv. Energy Mater. 2015, 5, 1501560 (Ref. 4)
LaTi <sub>0.65</sub> Fe <sub>0.35</sub> O <sub>3-<math>\delta</math></sub> /N-CNR	0.72	1.77	1.05	Nano Energy 2015, 15, 92 (Ref. 5).
La <sub>0.5</sub> Sr <sub>0.5</sub> Co <sub>0.8</sub> Fe <sub>0.2</sub> O <sub>3</sub> -PR/N- rGO	0.81	1.73	0.92	Nano Energy 2014, 10, 192 (Ref. 6).
La <sub>0.58</sub> Sr <sub>0.4</sub> Fe <sub>0.2</sub> Co <sub>0.8</sub> O <sub>3</sub> /N-CNT	0.7	1.63	0.93	Electrochimica Acta 2016, 208, 25 (Ref. 7).
Multi-shelled La <sub>0.9</sub> Sr <sub>0.1</sub> CoO <sub>3</sub>	0.64	1.76	1.12	J. Mater. Chem. A, 2015, 3, 22448 (Ref. 8).
NdBa <sub>0.5</sub> Sr <sub>0.5</sub> Co <sub>1.5</sub> Fe <sub>0.5</sub> O <sub>5+<math>\delta</math></sub> /CB	0.651	1.624	0.973	J. Mater. Chem. A, 2017, 5, 13019 (Ref. 9).
PrBa <sub>0.25</sub> Sr <sub>0.75</sub> Co <sub>2</sub> O <sub>5+<math>\delta</math></sub> /AB	0.68	1.65	0.97	Journal of Power Sources 2016, 334, 86 (Ref. 10).
Mn-oxide film	0.73	1.77	1.04	J. Am. Chem. Soc. 2010, 132, 13612 (Ref. 11).
Co <sub>3</sub> O <sub>4</sub> /N,S-doped carbon	0.82	1.61	0.79	Adv. Funct. Mater. 2014, 24, 7655 (Ref. 12).

MnO <sub>x</sub> on stainless steel mesh	0.82	1.62	0.8	Energy Environ. Sci. 2014, 7, 2017 (Ref. 13).
Mn <sub>x</sub> O <sub>y</sub> /N-doped Carbon	1.68	0.81	0.87	Angew. Chem. Int. Ed. 2014, 53, 8508 (Ref. 14).
CNT@NCNT	0.65	1.73	1.08	Adv. Funct. Mater. 2014, 24, 5956 (Ref. 15)
N-doped graphene/CNT	0.64	1.65	0.96	Small 2014, 10, 2251 (Ref. 16).
N,S,Fe-doped Carbon	0.87	1.78	0.91	J. Am. Chem. Soc. 2014, 136, 14486 (Ref. 17).
N-doped Carbon	0.77	1.61	0.84	Nat. Commun. 2013, 4, 2390 (Ref. 18).

## References

1. Z. Chen, A. Yu, D. Higgins, H. Li, H. Wang, Z. Chen, Highly Active and Durable Core–Corona Structured Bifunctional Catalyst for Rechargeable Metal–Air Battery Application, *Nano Lett.* 12 (2012) 1946-1952.
2. J.-I Jung, H.Y. Jeong, J.-S. Lee, M.G. Kim, J. Cho, A Bifunctional Perovskite Catalyst for Oxygen Reduction and Evolution, *Angew. Chem. Int. Ed.* 53 (2014) 4582-4586.
3. X. Han, F. Cheng, T. Zhang, J. Yang, Y. Hu, J. Chen, Hydrogenated Uniform Pt Clusters Supported on Porous CaMnO<sub>3</sub> as a Bifunctional Electrocatalyst for Enhanced Oxygen Reduction and Evolution, *Adv. Mater.* 26 (2014) 2047-2051.
4. J.-I. Jung, S. Park, M-G. Kim, J. Cho, Tunable Internal and Surface Structures of the Bifunctional Oxygen Perovskite Catalysts, *Adv. Energy Mater.* 5 (2015) 1501560.
5. M. Prabu, P. Ramakrishnan, P. Ganesan, A. Manthiram, S. Shanmugam, LaTi<sub>0.65</sub>Fe<sub>0.35</sub>O<sub>3-δ</sub> nanoparticle-decorated nitrogen-doped carbon nanorods as an advanced hierarchical air electrode for rechargeable metal-air batteries, *Nano Energy* 15 (2015) 92-103.

6. H.W. Park, D.U. Lee, P. Zamani, M.H. Seo, L.F. Nazar, Z. Chen, Electrospun porous nanorod perovskite oxide/nitrogen-doped graphene composite as a bi-functional catalyst for metal air batteries, *Nano Energy* 10 (2014) 192-200.
7. K. Elumeeva, J. Masa, J. Sierau, F. Tietz, M. Muhler, W. Schuhmann, Perovskite-based bifunctional electrocatalysts for oxygen evolution and oxygen reduction in alkaline electrolytes, *Electrochim. Acta* 208 (2016) 25-32.
8. S. Bie, Y. Zhu, J. Su, C. Jin, S. Liu, R. Yang, J. Wu, One-pot fabrication of yolk-shell structured  $\text{La}_{0.9}\text{Sr}_{0.1}\text{CoO}_3$  perovskite microspheres with enhanced catalytic activities for oxygen reduction and evolution reactions, *J. Mater. Chem. A* 3 (2015) 22448-22453.
9. N.-I. Kim, R.A. Afzal, S.R. Choi, S.W. Lee, D. Ahn, S. Bhattacharjee, S.-C. Lee, J.H. Kim, J.-Y. Park, Highly active and durable nitrogen doped-reduced graphene oxide/double perovskite bifunctional hybrid catalysts, *J. Mater. Chem. A* 5 (2017) 13019-13031.
10. Z. Wu, L.-P. Sun, T. Xia, L.-H. Huo, H. Zhao, A. Rougier, J.C. Grenier, Effect of Sr doping on the electrochemical properties of bi-functional oxygen electrode  $\text{PrBa}_{1-x}\text{Sr}_x\text{Co}_2\text{O}_{5+\delta}$ , *J. Power Sources* 334 (2016) 86-93.
11. Y. Gorlin, T.F. Jaramillo, A Bifunctional Nonprecious Metal Catalyst for Oxygen Reduction and Water Oxidation, *J. Am. Chem. Soc.* 132 (2010) 13612-13614.
12. C. Zhang, M. Antonietti, T.-P. Fellingner, Blood Ties:  $\text{Co}_3\text{O}_4$  Decorated Blood Derived Carbon as a Superior Bifunctional Electrocatalyst, *Adv. Funct. Mater.* 24 (2014) 7655-7665.
13. J.W.D. Ng, M. Tang, T.F. Jaramillo, A carbon-free, precious-metal-free, high-performance  $\text{O}_2$  electrode for regenerative fuel cells and metal-air batteries, *Energy Environ. Sci.* 7 (2014) 2017-2024.

14. J. Masa, W. Xia, I. Sinev, A. Zhao, Z. Sun, S. Grützke, P. Weide, M. Muhler, W. Schuhmann,  $Mn_xO_y/NC$  and  $Co_xO_y/NC$  Nanoparticles Embedded in a Nitrogen-Doped Carbon Matrix for High-Performance Bifunctional Oxygen Electrodes, *Angew. Chem. Int. Ed.* 53 (2014) 8508-8512.
15. G.-L. Tian, Q. Zhang, B. Zhang, Y.-G. Jin, J.-Q. Huang, D.S. Su, Toward Full Exposure of “Active Sites”: Nanocarbon Electrocatalyst with Surface Enriched Nitrogen for Superior Oxygen Reduction and Evolution Reactivity, *Adv. Funct. Mater.* 24 (2014) 5956-5961.
16. G.-L. Tian, M.-Q. Zhao, D. Yu, X.-Y. Kong, J.-Q. Q. Zhang, F. Wei, Nitrogen-Doped Graphene/Carbon Nanotube Hybrids: In Situ Formation on Bifunctional Catalysts and Their Superior Electrocatalytic Activity for Oxygen Evolution/Reduction Reaction, *small* 10 (2014) 2251-2259.
17. N.R. Ashraie, J.P. Paraknowitsch, C. Göbel, A. Thomas, P. Strasser, Noble-Metal-Free Electrocatalysts with Enhanced ORR Performance by Task-Specific Functionalization of Carbon using Ionic Liquid Precursor Systems, *J. Am. Chem. Soc.* 136 (2014) 14486-14497.
18. Y. Zhao, R. Nakamura, K. Kamiya, S. Nakanishi, K. Hashimoto, Nitrogen-doped carbon nanomaterials as non-metal electrocatalysts for water oxidation, *Nat. Commun.*, 4 (2013) 2390.